Submitted: 06 October, 2023 Accepted: 21 November, 2023 Published: 30 May, 2024 DOI:10.22514/jomh.2024.070

ORIGINAL RESEARCH

JOMH Journal of Men's Health

A nomogram for predicting extraprostatic extension in prostate cancer based on extraprostatic extension grade and clinical characteristics

Quan Ma[1,†], Wei Tian[1,†], Shasha Lv[2], Yongna Fu[2], Hui Wang[3], Jiansong He[1], Yongliang Chen[1,*]

[1]Department of Urology, Shaoxing Central Hospital, 312000 Shaoxing, Zhejiang, China
[2]Department of Radiology, Shaoxing Central Hospital, 312000 Shaoxing, Zhejiang, China
[3]Department of Pathology, Shaoxing Central Hospital, 312000 Shaoxing, Zhejiang, China

***Correspondence**
sxcentral@stu.hebmu.edu.cn
(Yongliang Chen)

† These authors contributed equally.

Abstract

To assess the efficacy of a nomogram model derived from extraprostatic extension (EPE) grade on magnetic resonance imaging (MRI) and clinical features in forecasting pathological EPE in prostate cancer. We conducted a retrospective analysis of the clinical data from 232 prostate cancer patients. Patients were categorized into EPE and non-EPE groups based on the presence of pathological EPE. Subsequently, they were randomly allocated into a training set (162 cases) and a validation set (70 cases) at a 7:3 ratio. We gathered clinical attributes and EPE grades for all patients. Three predictive models—clinic, magnetic resonance (MR) and clinic + MR—were developed within the training set. The clinic + MR model was visualized through a nomogram. The models' performance was assessed using the receiver operating characteristic (ROC) curve, calibration curve, and decision curve analysis (DCA). Both univariate and multivariate logistic regression analyses identified the biopsy International Society of Urological Pathology (ISUP) category and biopsy maximum unilateral positive percentage as independent risk factors for EPE within the training set. The EPE grade exhibited consistent inter-observer agreement, evidenced by weighted Kappa values of 0.72 and 0.71 in the training and validation sets, respectively. Compared to the clinic and MR models, the clinic + MR model was the most effective in predicting pathological EPE, boasting area under the curves (AUCs) of 0.85 and 0.82 in the training and validation sets, respectively. Calibration curves from both sets demonstrated that the clinic + MR model provided accurate predictions for pathological EPE. Within the DCA, the clinic + MR model surpassed the clinic and MR models in terms of clinical net benefit in both sets. The clinic + MR model excels in predicting the pathological EPE of prostate cancer. Its superiority over the clinic model underscores its clinical relevance and the potential for broader implementation.

Keywords

Extraprostatic extension; Prostate cancer; Magnetic resonance imaging; Nomogram; Diagnostic performance

1. Introduction

Prostate cancer is a common malignant tumor that affects the male genitourinary system. Globally, its incidence and mortality rates rank second and fifth, respectively, among male neoplasms [1]. Compared to localized prostate cancer, extraprostatic extension (EPE) is associated with higher incidences of positive surgical margins and biochemical recurrence, often requiring additional adjuvant therapy. Furthermore, EPE is intrinsically linked to disease progression and adverse prognosis [2, 3]. Radical prostatectomy (RP) is a primary treatment option for prostate cancer [4]. While RP effectively manages prostate cancer, it comes with notable complications, such as erectile dysfunction and urinary incontinence [5, 6], which profoundly impact patients' quality of life. For those without EPE, nerve-sparing RP offers an avenue to enhance sexual function and urinary continence without compromising the integrity of surgical margins [7]. Thus, accurate preoperative determination of EPE is critical for informed clinical decision-making and optimal surgical planning.

Magnetic resonance imaging (MRI) serves as the foremost technique for the preoperative prediction of EPE. The Prostate Imaging Reporting and Data System (PI-RADS) provides a comprehensive framework for assessing the imaging characteristics of EPE [8]. Yet, its diagnostic efficacy is limited by the lack of a quantitative evaluation of these characteristics [9]. The Likert scale amalgamates the imaging traits of EPE, as detailed in PI-RADS, classifying the likelihood

of EPE into five categories. Nevertheless, due to its lack of objective criteria, this scale exhibits considerable variability in diagnostic accuracy [10–12]. In 2019, Mehralivand *et al.* [13] introduced a standardized, streamlined EPE grade system that amalgamates both qualitative and quantitative MRI indicators. At present, validation studies focusing on the EPE grade remain sparse, especially concerning the Chinese demographic.

Consequently, this research undertook a retrospective analysis of the clinical data from prostate cancer patients treated at Shaoxing Central Hospital between January 2018 and October 2022. Our objectives were to ascertain the diagnostic precision of the EPE grade in predicting pathological EPE and to gauge inter-observer concordance. In tandem, we crafted a clinic + MR model by amalgamating the EPE grade with pertinent clinical and pathological data, aiming to evaluate its diagnostic prowess in predicting pathological EPE.

2. Materials and methods

2.1 Study population

Clinical and pathological data were retrospectively gathered from patients who underwent laparoscopic radical prostatectomy for prostate cancer at the Department of Urology, Shaoxing Central Hospital, between January 2018 and October 2022. Inclusion criteria were: (1) Pathological diagnosis of prostate cancer; (2) Preoperative prostate MRI examination. Exclusion criteria included: (1) Preoperative MRI for more than 6 months or MRI at an outside institution (n = 12); (2) Adjuvant therapy such as chemotherapy and endocrine therapy before surgery (n = 5); (3) Presence of artifacts on prostate MRI (n = 3); (4) Inadequate clinical information (n = 15). A total of 232 prostate cancer patients were considered for this study. Out of them, 103 exhibited a pathological EPE post-surgery, translating to an EPE incidence rate of 44.40%. These patients were then randomly assigned into a training set (n = 162) and a validation set (n = 70) at a 7:3 ratio (Fig. 1).

2.2 Clinical information

Collected data encompassed clinical, laboratory, MRI and pathological details, which included age, Total Prostate Specific Antigen (TPSA), Free Prostate Specific Antigen (FPSA), prostate volume, Prostate Specific Antigen Density (PSAD), biopsy Gleason score, biopsy International Society of Urological Pathology (ISUP) category, biopsy maximum unilateral positive percentage, biopsy total positive percentage, and EPE grade of prostate MRI.

2.3 EPE grade on MRI

All MRIs were conducted using a 1.5T MRI scanner (Philips, Amsterdam, Netherlands). The imaging protocols incorporated axial and sagittal T1-weighted imaging (T1WI), T2-weighted imaging (T2WI), and diffusion weighted imaging (DWI). Corresponding apparent diffusion coefficient (ADC) maps were computed by b-values of 0 and 800 mm^2/s. The EPE grade system, based on Mehralivan *et al.* [13], was employed as follows: grade 0, no suspicion for EPE; grade 1, either curvilinear contact length (CCL) $\geq$1.5 cm or capsular irregularity and bulge; grade 2, both CCL $\geq$1.5 cm and capsular irregularity and bulge; grade 3, frank EPE visible at MRI or invasion of adjacent anatomic structures. Two experienced radiologists, with 10 and 5 years of prostate MRI expertise respectively, assigned the EPE grades without prior knowledge of the prostate pathology. Consensus EPE grades were documented, in instances of disagreement, a mutually agreed-upon grade was finalized.

2.4 Pathological diagnosis of prostate cancer

Following radical prostatectomy, pathological specimens were appropriately preserved in a 10% neutral formaldehyde solution and subsequently stained using hematoxylin and eosin for both the surgical margins and prostate tissues. Sections were consistently taken at intervals of 2–3 mm, aligned perpendicular to the gland's long (apical-basal) axis. An adept pathologist assessed these sections, identifying the lesion and confirming the presence or absence of EPE. Both the Gleason score and ISUP category for the lesion were documented in accordance with the 2019 edition of the ISUP guidelines [14].

2.5 Statistical analysis

Statistical evaluations were conducted using SPSS (version 19.0, IBM Corporation, Armonk, NY, USA) and R software (version 4.2.3, R Development Core Team, Vienna, Austria). Data following a normal distribution were denoted as $\bar{x} \pm s$, while data with a skewed distribution were presented as M (Q1, Q3). To compare between groups, the independent samples *t*-test or the Mann-Whitney U-test was employed. For count data group comparisons, the χ^2 test or Fisher's exact probability method was utilized. The consistency between observation groups was determined using the weighted Kappa test, with weighted Kappa values categorized as: $<$0.21 (poor), $\geq$0.21–0.41 (fair), $\geq$0.41–0.61 (moderate), $\geq$0.61–0.81 (good), and $\geq$0.81–1.00 (very good). Both univariate and multivariate logistic regression analyses were employed to identify clinical risk factors associated with pathological EPE in post-surgery prostate cancer patients within the training set. Based on these identified risk factors, a clinic model was established. A separate MR model, reliant on the MRI-determined EPE grade, was also constructed for the training set. By integrating the clinical risk factors with the EPE grade, a combined clinic + MR model was developed to predict pathological EPE in the training set. This integrated model was visualized as a nomogram. The respective ROC curves of the three models were graphed, the AUC was calculated, and the DeLong test discerned differences among these models. Calibration curves evaluated the clinic + MR model's calibration, and DCA gauged the models' net clinical benefits. A *p*-value of less than 0.05 was considered indicative of statistical significance.

3. Results

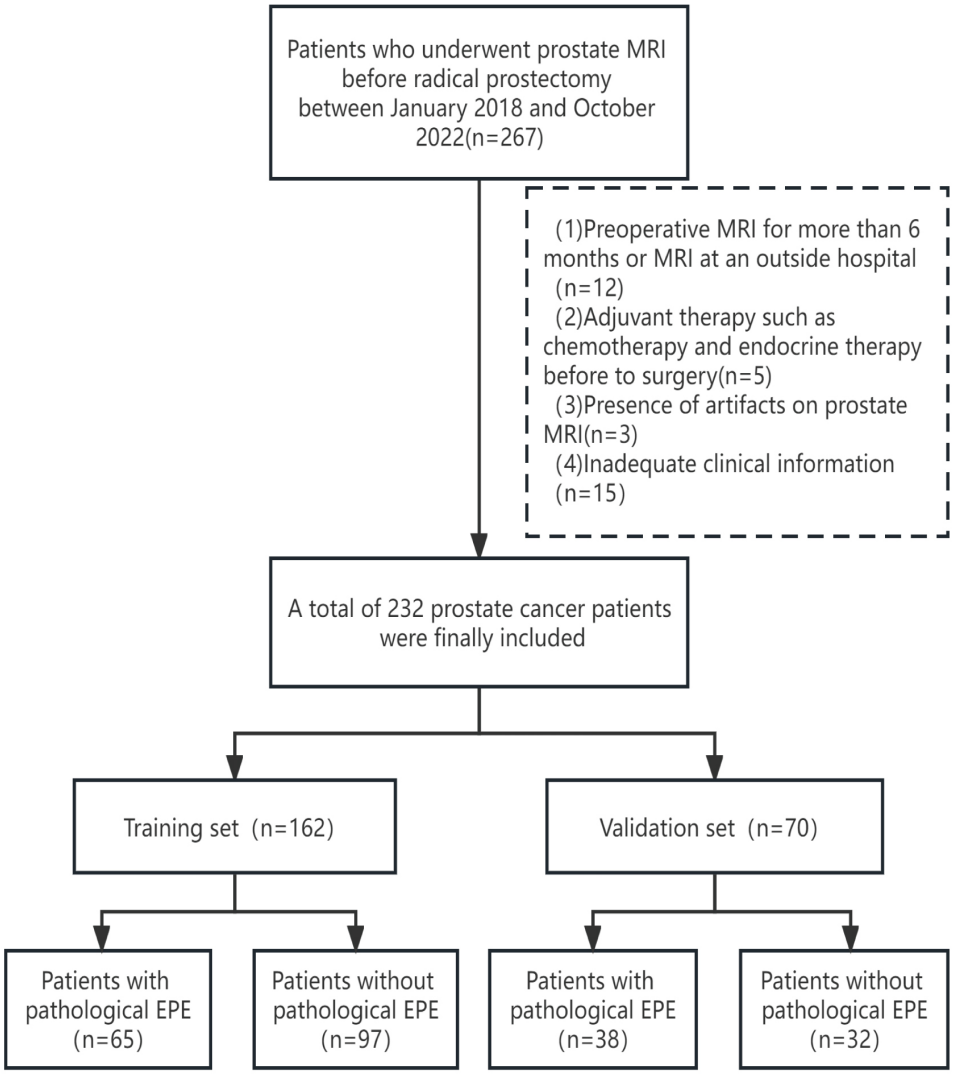

FIGURE 1. Flow diagram of patient selection and randomization grouping for the study. EPE: extraprostatic extension; MRI: magnetic resonance imaging.

3.1 Clinical characteristics

A comparison of clinical characteristics between EPE and non-EPE groups within the training set is detailed in Table 1. Distinct variables including age, TPSA, PSAD, biopsy Gleason score, biopsy ISUP category, biopsy maximum unilateral positive percentage, biopsy total positive percentage were statistically significant ($p < 0.05$). Within the training set, EPE patients exhibited notably elevated values for age, PSA and PSAD in contrast to non-EPE patients ($p < 0.05$). The biopsy Gleason score, biopsy ISUP category, biopsy maximum unilateral positive percentage, and biopsy total positive percentage also demonstrated significant variations between EPE and non-EPE groups ($p < 0.05$) (Table 1).

3.2 Univariate and multivariate logistic regression analyses of pathological EPE after prostate cancer surgery

Both clinical and pathological features (age, TPSA, FPSA, prostate volume, PSAD, biopsy Gleason score, biopsy ISUP category, biopsy maximum unilateral positive percentage and biopsy total positive percentage) were incorporated into the univariate and multivariate logistics regression analyses. The biopsy ISUP category and biopsy maximum unilateral positive percentage emerged as independent clinical risk factors for pathological EPE post-prostate cancer surgery, as shown in Table 2.

3.3 EPE grade on MRI

Statistically significant discrepancy in the EPE grade was observed between the EPE and non-EPE sets in the training set ($p < 0.05$) (Table 1). Both evaluators displayed commendable consistency in the EPE grade, boasting weighted Kappa values of 0.72 (95% CI: 0.65–0.80) and 0.71 (95% CI: 0.58–0.83) in the training and validation sets respectively.

3.4 Predictive models

In the training set, two clinical features (biopsy ISUP category and biopsy Maximum unilateral positive percentage) were leveraged to devise a clinic model predicting pathological EPE, resulting in AUC values of 0.80 and 0.76 for the training and

TABLE 1. Characteristics of EPE and non-EPE groups in the training set.

Parameters	EPE group (n = 65)	Non-EPE group (n = 97)	Statistical value	*p*-value
Age (year)*	75.91 ± 5.60	73.68 ± 6.01	−2.375[b]	0.019
TPSA (ng/mL)‡	15.47 (8.99, 32.88)	8.73 (6.66, 14.00)	−4.294[c]	<0.001
FPSA (ng/mL)‡	1.43 (1.06, 3.08)	1.37 (0.92, 2.28)	−1.093[c]	0.274
Prostate volume (cm^3)*	36.42 ± 15.30	41.80 ± 18.37	1.949[b]	0.053
PSAD (ng/mL^2)‡	0.58 (0.28, 0.93)	0.22 (0.16, 0.41)	−5.371[c]	<0.001
Biopsy Gleason score n (%)				
6	11 (16.92%)	51 (52.58%)		
7	21 (32.31%)	30 (30.93%)		
8	19 (29.23%)	11 (11.34%)	29.114[a]	<0.001
9	11 (16.92%)	3 (3.09%)		
10	3 (4.62%)	2 (2.06%)		
Biopsy ISUP category n (%)				
1	11 (16.92%)	51 (52.58%)		
2	14 (21.54%)	24 (24.74%)		
3	7 (10.77%)	6 (6.19%)	29.751[a]	<0.001
4	19 (29.23%)	11 (11.34%)		
5	14 (21.54%)	5 (5.15%)		
Maximum unilateral positive percentage at biopsy n (%)				
<34%	13 (20%)	59		
34–67%	13 (20%)	22	36.421[a]	<0.001
>67%	39 (60%)	16		
Total positive percentage at biopsy n (%)				
<34%	19	73		
34–67%	30	19	34.97[a]	<0.001
>67%	16	5		
EPE grade n (%)				
0	18	75		
1	20	11	39.567[a]	<0.001
2	16	6		
3	11	5		

*Abbreviations: TPSA: Total Prostate Specific Antigen; FPSA: Free Prostate Specific Antigen; PSAD: Prostate Specific Antigen Density; ISUP: International Society of Urological Pathology; EPE: extraprostatic extension. *Data are mean ± standard deviation. ‡Data are mean, and data in parentheses are the interquartile spacing. [a]Data are chi-square. [b]Data are t-value. [c]Data are z-value.*

validation sets respectively (Table 3). Utilizing the EPE grade on MRI from the training set, the MR model was formulated, producing AUCs of 0.75 and 0.77 in the training and validation sets respectively (Table 3). The clinic + MR model was established incorporating three parameters: biopsy ISUP category, biopsy maximum unilateral positive percentage, and EPE grade from the training set; this model yielded AUCs of 0.85 and 0.82 for the training and validation sets respectively (Table 3). The ROC curves for the trio of models are illustrated in Fig. 2. Relative to the clinic model, the clinic + MR model markedly augmented diagnostic efficacy in both the training set (clinic *vs.* clinic + MR, $p = 0.029$) and validation set (clinic *vs.* clinic + MR, $p = 0.035$). A corresponding nomogram for the clinic + MR model is depicted in Fig. 3. Calibration curves confirmed the clinic + MR model's adept calibration for predicting pathological EPE (Fig. 4), with the Hosmer-Lemeshow test rendering non-significant results ($p = 0.472$ for training set, $p = 0.669$ for validation set). In the decision curve analysis, the clinic + MR model outperformed both the clinic and MR models in terms of net clinical benefit (Fig. 5).

TABLE 2. Univariate and multivariate logistic regression analysis of pathological EPE after prostate cancer surgery.

Parameters	Univariate logistic regression analysis		Multivariate logistic regression analysis	
	OR (95% CI)	*p* value	OR (95% CI)	*p* value
Age	1.068 (1.010–1.129)	0.021	-	-
TPSA	1.030 (1.006–1.054)	0.013	-	-
FPSA	1.031 (0.973–1.093)	0.306	-	-
Prostate volume	0.981 (0.962–1.001)	0.057	-	-
PSAD	4.796 (1.895–12.142)	0.001	-	-
Biopsy Gleason score	2.291 (1.621–3.239)	<0.001	-	-
Biopsy ISUP category	1.910 (1.489–2.451)	<0.001	1.588 (1.209–2.085)	0.001
Biopsy maximum unilateral positive percentage	3.335 (2.192–5.076)	<0.001	2.606 (1.666–4.075)	<0.001
Total positive percentage at biopsy	4.216 (2.463–7.215)	<0.001	-	-

TPSA: Total Prostate Specific Antigen; FPSA: Free Prostate Specific Antigen; PSAD: Prostate Specific Antigen Density; ISUP: International Society of Urological Pathology; OR: odds ratio; CI: confidence interval; -: Data is not measured.

TABLE 3. Statistical indicators of predictive models.

models	AUC	Sensitivity	Specificity	Accuracy
Clinic model in training set	0.80	0.65	0.87	0.78
Clinic model in validation set	0.76	0.82	0.66	0.74
MR model in training set	0.75	0.72	0.77	0.75
MR model in validation set	0.77	0.76	0.78	0.77
Clinic + MR model in training set	0.85	0.89	0.73	0.80
Clinic + MR model in validation set	0.82	0.82	0.78	0.80

AUC: area under the curve; MR: magnetic resonance.

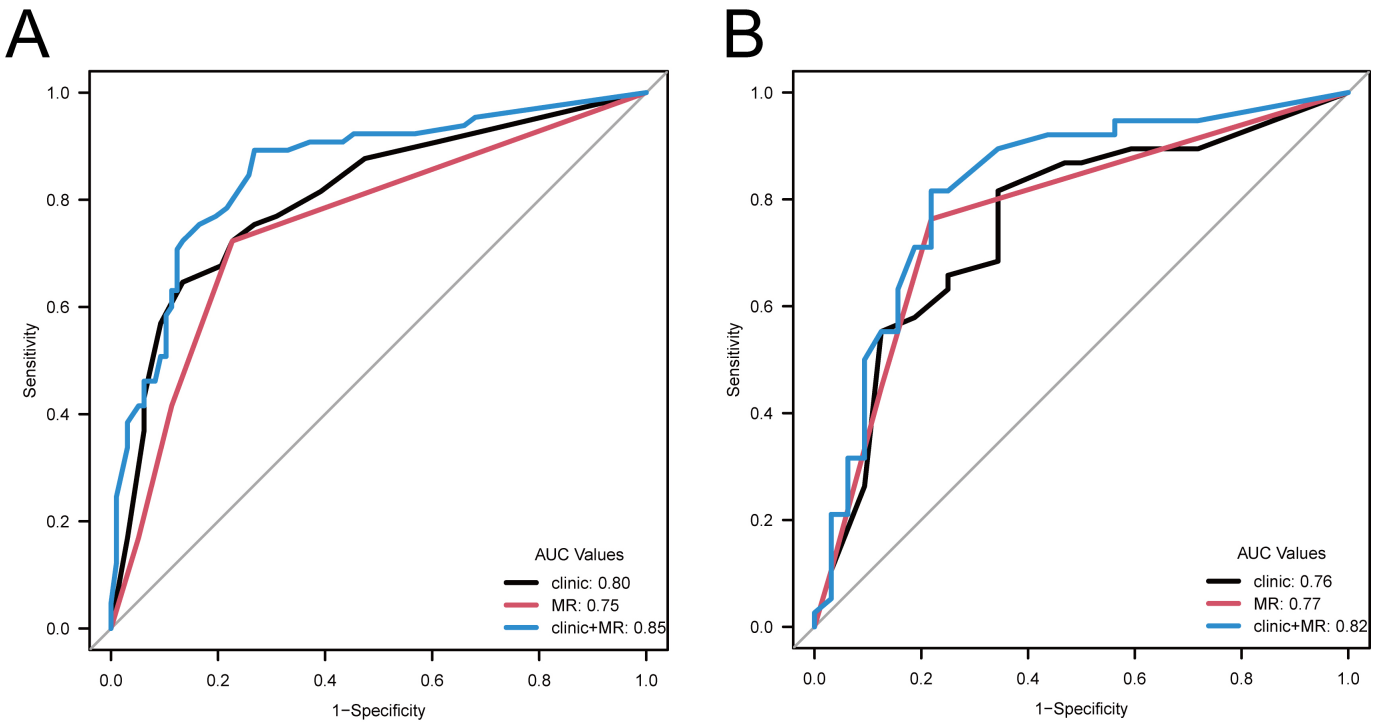

FIGURE 2. ROC curves of models in the training and validation sets. (A) ROC curves of the clinic model, MR model, and clinic + MR model in the training set. (B) ROC curves of the clinic model, MR model, and clinic + MR model in the validation set. AUC: area under the curve; MR: magnetic resonance.

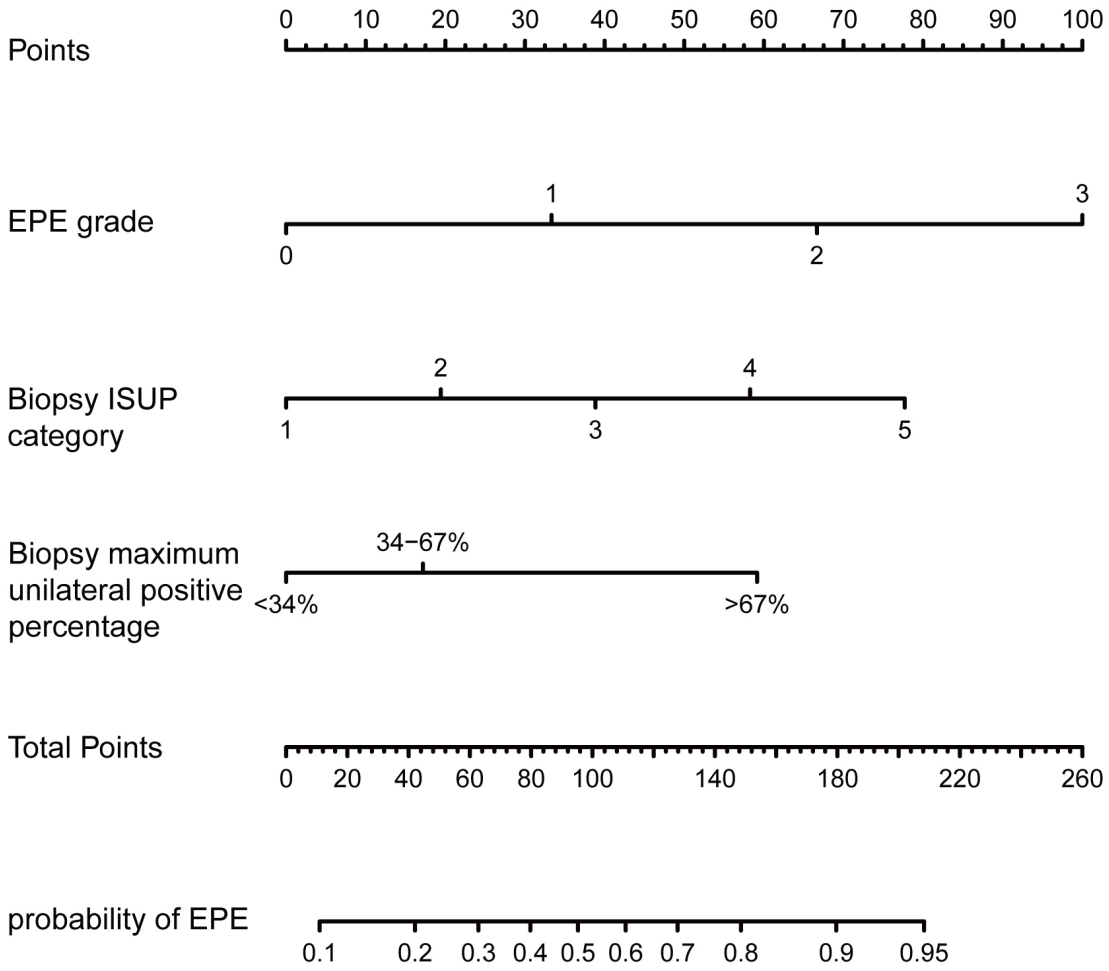

FIGURE 3. The nomogram of the clinic + MR model. EPE: extraprostatic extension; ISUP: International Society of Urological Pathology.

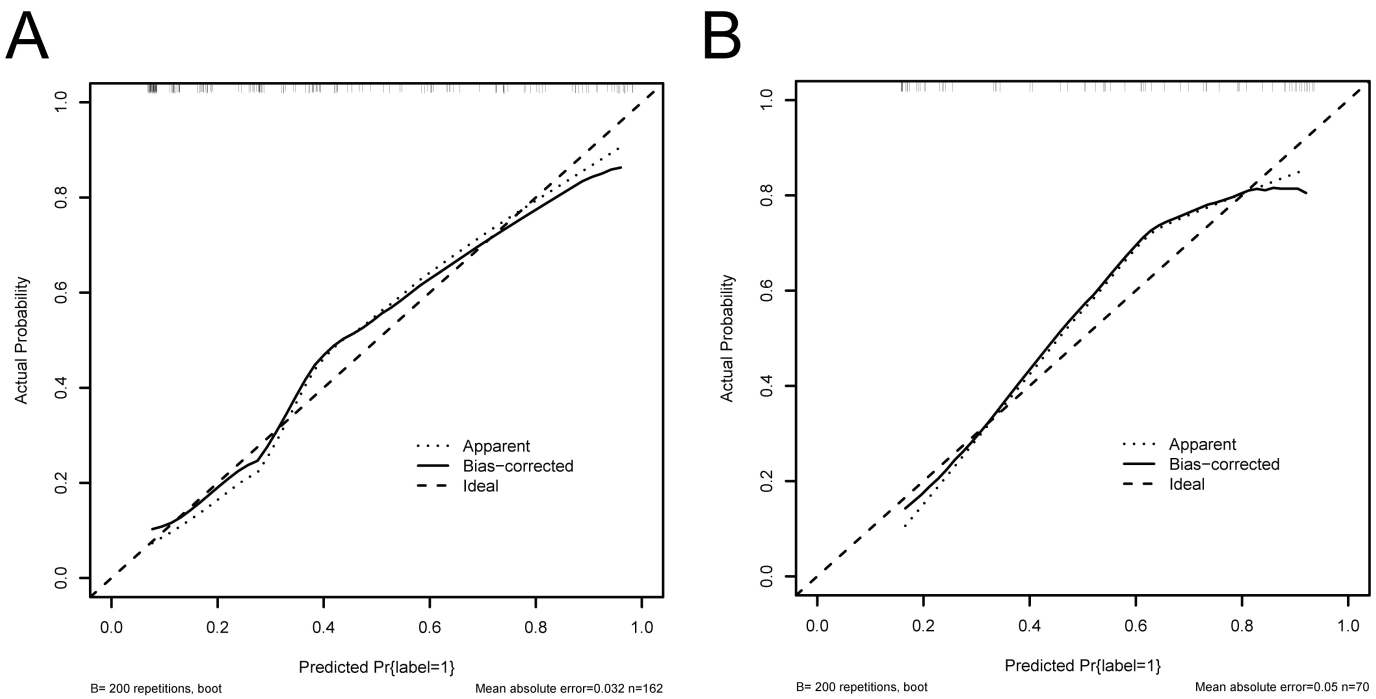

FIGURE 4. Calibration curves of the clinic + MR model. (A) Calibration curves of the clinic + MR model in the training set. (B) Calibration curves of the clinic + MR model in the validation set.

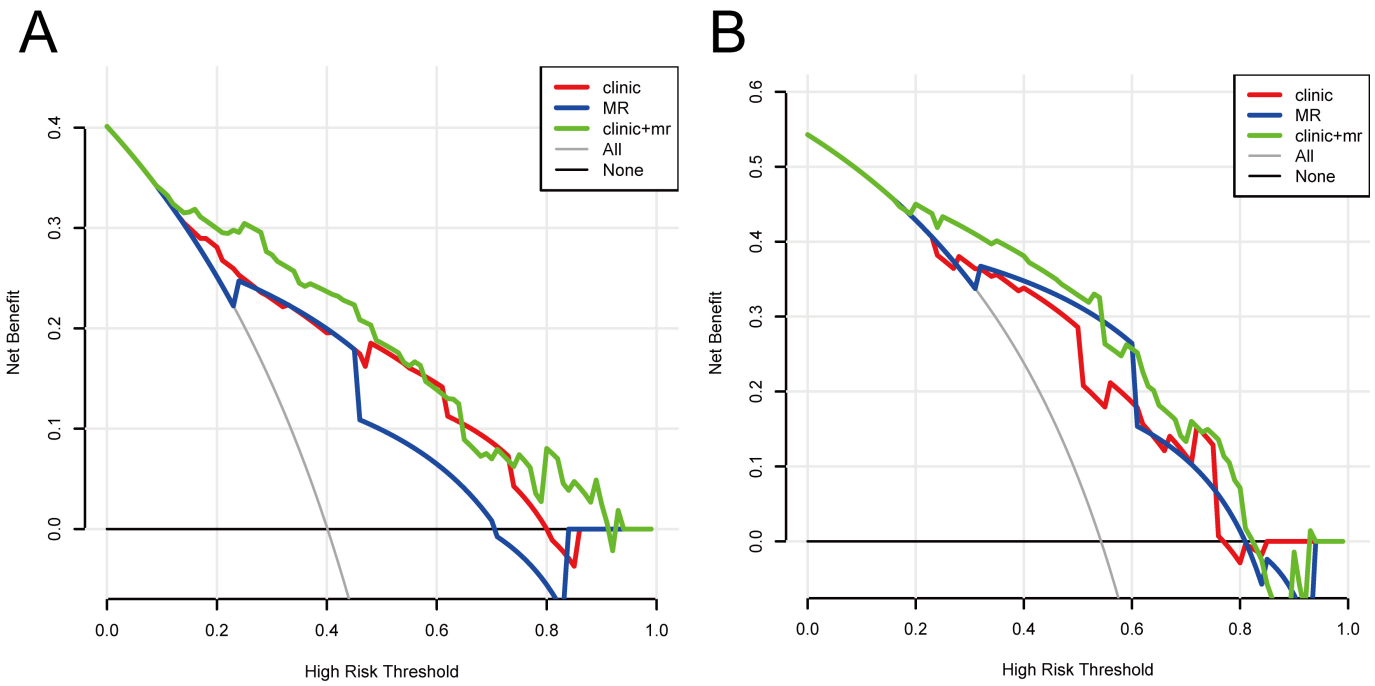

FIGURE 5. Decision curve analysis of models. (A) Decision curve analysis of the clinic model, MR model, and clinic + MR model in the training set. (B) Decision curve analysis of the clinic model, MR model, and clinic + MR model in the validation set. MR: magnetic resonance.

4. Discussion

In this study, we developed an MR model based on the EPE grade derived from MRI, demonstrating both robust diagnostic efficacy and consistent inter-observer agreement. This clinic model was formulated to predict pathological EPE, drawing on biopsy ISUP category and biopsy maximum unilateral positive percentage. Using the biopsy ISUP category, biopsy maximum unilateral positive percentage, and EPE grade from MRI, we crafted the clinic + MR model. Subsequently, we employed nomogram visualization. This clinic + MR model surpasses both the pure MR model and the clinical model in terms of diagnostic efficacy and clinical net benefit.

MRI provides added value in predicting pathological EPE. A meta-analysis indicated that while MRI boasts a specificity of 0.91, its sensitivity is a mere 0.57 for predicting pathological EPE [15]. Although the European Society of Urogenital Radiology (ESUR) scores and Likert scales are utilized to assess pathological EPE, their absence of objective indicators compromises reproducibility. Current studies validate that CCL stands as an autonomous predictor of pathological EPE, showcasing impressive sensitivity and inter-observer agreement [16–18]. Accordingly, the EPE grade introduced by Mehralivand *et al.* [13] omits intricate qualitative descriptors, saving for capsular irregularity or bulge. It also integrates quantitative attributes for a CCL $\geq$15 mm. Park *et al.* [16] reinforced the diagnostic efficacy of the EPE grade, noting a sensitivity between 77.5% and 79.8%, an AUC between 0.77 and 0.81, and the most potent association with pathological EPE relative to ESUR scores and Likert scales. The EPE grade, encompassing both qualitative and quantitative factors, minimizes reliance on observer expertise. Its weighted kappa, ranging from 0.647 to 0.71 for inter-observer agreement, eclipses that of the ESUR scores and Likert scales, which are strictly qualitative [16, 17]. A recent inquiry deduced that the EPE grade possesses marked diagnostic efficacy in anticipating the biochemical recurrence of prostate cancer [19]. Within our study, the weighted kappa scores for the EPE grade in the training and validation groups stood at 0.72 and 0.71, respectively. The participating radiologists, representing both junior and senior levels, achieved remarkable inter-observer congruence. This suggests that the EPE grade, demanding minimal MRI reading experience, is apt for both reporting and instruction. Echoing prior research, our study's AUC values for the training and validation sets were 0.75 and 0.77, with sensitivities of 0.72 and 0.76, respectively, further externalizing the diagnostic efficacy of the EPE grade.

Several clinical models, including the Partin tables, Cancer of the Prostate Risk Assessment (CAPRA) score, and the Memorial Sloan Kettering Cancer Center (MSKCC) nomogram [20, 21], have been employed to forecast pathological EPE. However, these models primarily draw on data from European and American demographics and notably exclude the biopsy ISUP category. The ISUP category boasts superior prognostic accuracy relative to the Gleason score [22]. Moreover, both the biopsy ISUP category and biopsy positive percentage are recognized as distinct risk determinants for pathological EPE, reflecting AUC values of 0.796 and 0.762, respectively [23]. In our research, we adopted the highest grade for the biopsy ISUP category due to its enhanced predictive capacity concerning the stage and grade of prostate cancer [24]. Additionally, we separately quantified the positive percentages for the left and right lateral lobes, selecting the greater value as the biopsy maximum unilateral positive percentage. A clinical model was designed around the biopsy ISUP category and biopsy maximum unilateral positive percentage, presenting

AUC values of 0.8 and 0.76 in the training and validation sets, respectively—aligning with prior studies. Yet, we discerned significant volatility in the sensitivity and specificity across the training and validation sets, which might be attributed to the clinical model's diminished reliability during internal validation [25]. Thus, there's a pressing need to devise a more potent and consistent prediction model, potentially through the incorporation of additional markers.

In recent years, numerous researchers have sought to amalgamate the EPE grade with clinical and pathological characteristics to craft a composite model for predicting pathological EPE, endeavoring to refine predictive effectiveness. Mehralivand *et al.* [13] formulated a clinical model utilizing log PSA and biopsy ISUP category, achieving an AUC of 0.77. Yet, when merged with the EPE grade, the AUC ascended to 0.81. Xu *et al.* [26] similarly validated that merging the EPE grade with clinical traits considerably elevated the diagnostic proficiency of the clinical model. Furthermore, this integrated model exhibited superior calibration prowess and clinical net advantage. A contemporaneous study inferred that the model incorporating the EPE grade potentially surpasses the efficacy of PI-RADS V2.1, with AUC values standing at 0.879 and 0.802, respectively [27]. In our endeavor, we fashioned a clinic + MR model for predicting pathological EPE by assimilating the EPE grade and biopsy pathological metrics. This model's nomogram visualization displayed an AUC of 0.85, a value significantly higher than that of the standalone clinical model. Our internal validation yielded an AUC of 0.82 for the validation set. Moreover, the clinic + MR model demonstrated enhanced calibration and clinical net benefit in both training and validation sets.

This study presents several limitations. First, it is retrospective in nature, introducing potential selection bias. Second, it is confined to a single centre and encompasses a limited sample size. Lastly, the study lacks external validation data, necessitating further data acquisition to ascertain the predictive model's robustness.

5. Conclusions

The EPE grade showcases commendable diagnostic efficacy and inter-observer consistency, hinting at its augmented predictive value for pathological EPE. The clinic + MR model, integrating biopsy ISUP category, biopsy maximum unilateral positive percentage, and EPE grade, exhibits pronounced predictive acumen for pathological EPE. As delineated by the clinic + MR model's nomogram, it facilitates the estimation of pathological EPE likelihood, making it an invaluable tool for clinical decision-making and meriting broader adoption.

ABBREVIATIONS

EPE, extraprostatic extension; ROC, received operating characteristic; AUC, area under the curve; DCA, decision curve analysis; ISUP, International Society of Urological Pathology; MRI, Magnetic resonance imaging; MR, magnetic resonance; PI-RADS, Prostate Imaging Reporting and Data System; TPSA, Total Prostate Specific Antigen; FPSA, Free Prostate Specific Antigen; PSAD, Prostate Specific Antigen Density; T1WI, T1-weighted imaging; T2WI, T2-weighted imaging; DWI, diffusion weighted imaging; ADC, apparent diffusion coefficient; CCL, curvilinear contact length; ESUR, European Society of Urogenital Radiology; CAPRA, Cancer of the Prostate Risk Assessment; MSKCC, Memorial Sloan Kettering Cancer Center.

AVAILABILITY OF DATA AND MATERIALS

The data presented in this study are available on reasonable request from the corresponding author.

AUTHOR CONTRIBUTIONS

YLC—guarantor of the article. YLC and QM—conception and design. WT, SSL, YNF and HW—collection and assembly of data. QM, WT, SSL, YNF, HW and JSH—data analysis and interpretation. QM and HW—writing manuscript. All authors have collaboratively contributed to and endorsed the final manuscript.

ETHICS APPROVAL AND CONSENT TO PARTICIPATE

Research involving human participants were reviewed and approved by Institutional Review Board of Shaoxing Central Hospital (2023-037). The Medical Ethics Committee of Shaoxing Central Hospital approved this research, and informed consent from patients was waived.

ACKNOWLEDGMENT

Not applicable.

FUNDING

This research received no external funding.

CONFLICT OF INTEREST

The authors declare no conflict of interest.

REFERENCES

[1] Sung H, Ferlay J, Siegel RL, Laversanne M, Soerjomataram I, Jemal A, *et al*. Global cancer statistics 2020: GLOBOCAN estimates of incidence and mortality worldwide for 36 cancers in 185 countries. CA: A Cancer Journal for Clinicians. 2021; 71: 209–249.

[2] Numbere N, Teramoto Y, Gurung PMS, Goto T, Yang Z, Miyamoto H. The clinical impact of pT3a lesions in patients with pT3b prostate cancer undergoing radical prostatectomy. Archives of Pathology & Laboratory Medicine. 2022; 146: 619–625.

[3] Jeong BC, Chalfin HJ, Lee SB, Feng Z, Epstein JI, Trock BJ, *et al*. The relationship between the extent of extraprostatic extension and survival following radical prostatectomy. European Urology. 2015; 67: 342–346.

[4] Zhu Z, Zhu Y, Xiao Y, Hu S. Indications for nerve-sparing surgery for radical prostatectomy: results from a single-center study. Frontiers in Oncology. 2022; 12: 896033.

[5] Morozov A, Barret E, Veneziano D, Grigoryan V, Salomon G, Fokin I,

et al. A systematic review of nerve-sparing surgery for high-risk prostate cancer. Minerva Urology and Nephrology. 2021; 73: 283–291.

[6] Moretti TBC, Magna LA, Reis LO. Continence criteria of 193618 patients after open, laparoscopic, and robot-assisted radical prostatectomy. To be published in BJU International. 2023. [Preprint].

[7] Görgen ARH, Burttet LM, Cachoeira ET, Knijnik PG, Brum PW, De Oliveira Paludo A, *et al*. Association of nerve-sparing grading in robotic radical prostatectomy and trifecta outcome. World Journal of Urology. 2022; 40: 2925–2930.

[8] Turkbey B, Rosenkrantz AB, Haider MA, Padhani AR, Villeirs G, Macura KJ, *et al*. Prostate imaging reporting and data system version 2.1: 2019 update of prostate imaging reporting and data system version 2. European Urology. 2019; 76: 340–351.

[9] Schieda N, Quon JS, Lim C, El-Khodary M, Shabana W, Singh V, *et al*. Evaluation of the European society of urogenital radiology (ESUR) PI-RADS scoring system for assessment of extra-prostatic extension in prostatic carcinoma. European Journal of Radiology. 2015; 84: 1843–1848.

[10] Costa DN, Passoni NM, Leyendecker JR, de Leon AD, Lotan Y, Roehrborn CG, *et al*. Diagnostic utility of a likert scale versus qualitative descriptors and length of capsular contact for determining extraprostatic tumor extension at multiparametric prostate MRI. American Journal of Roentgenology. 2018; 210: 1066–1072.

[11] Freifeld Y, Diaz de Leon A, Xi Y, Pedrosa I, Roehrborn CG, Lotan Y, *et al*. Diagnostic performance of prospectively assigned likert scale scores to determine extraprostatic extension and seminal vesicle invasion with multiparametric MRI of the prostate. American Journal of Roentgenology. 2019; 212: 576–581.

[12] Fütterer JJ, Engelbrecht MR, Huisman HJ, Jager GJ, Hulsbergen-van De Kaa CA, Witjes JA, *et al*. Staging prostate cancer with dynamic contrast-enhanced endorectal MR imaging prior to radical prostatectomy: experienced versus less experienced readers. Radiology. 2005; 237: 541–549.

[13] Mehralivand S, Shih JH, Harmon S, Smith C, Bloom J, Czarniecki M, *et al*. A grading system for the assessment of risk of extraprostatic extension of prostate cancer at multiparametric MRI. Radiology. 2019; 290: 709–719.

[14] van Leenders GJLH, van der Kwast TH, Grignon DJ, Evans AJ, Kristiansen G, Kweldam CF, *et al*. The 2019 international society of urological pathology (ISUP) consensus conference on grading of prostatic carcinoma. American Journal of Surgical Pathology. 2020; 44: e87–e99.

[15] de Rooij M, Hamoen EHJ, Witjes JA, Barentsz JO, Rovers MM. Accuracy of magnetic resonance imaging for local staging of prostate cancer: a diagnostic meta-analysis. European Urology. 2016; 70: 233–245.

[16] Park KJ, Kim M, Kim JK. Extraprostatic tumor extension: comparison of preoperative multiparametric MRI criteria and histopathologic correlation after radical prostatectomy. Radiology. 2020; 296: 87–95.

[17] Asfuroğlu U, Asfuroğlu BB, Özer H, Gönül İİ, Tokgöz N, İnan MA, *et al*. Which one is better for predicting extraprostatic extension on multiparametric MRI: ESUR score, Likert scale, tumor contact length, or EPE grade? European Journal of Radiology. 2022; 149: 110228.

[18] Kongnyuy M, Sidana A, George AK, Muthigi A, Iyer A, Ho R, *et al*. Tumor contact with prostate capsule on magnetic resonance imaging: a potential biomarker for staging and prognosis. Urologic Oncology: Seminars and Original Investigations. 2017; 35: 30.e1–30.e8.

[19] Reisæter LAR, Halvorsen OJ, Beisland C, Honoré A, Gravdal K, Losnegård A, *et al*. Assessing extraprostatic extension with multiparametric MRI of the prostate: mehralivand extraprostatic extension grade or extraprostatic extension likert scale? Radiology: Imaging Cancer. 2020; 2: e190071.

[20] Eissa A, Elsherbiny A, Zoeir A, Sandri M, Pirola G, Puliatti S, *et al*. Reliability of the different versions of Partin tables in predicting extraprostatic extension of prostate cancer: a systematic review and meta-analysis. Minerva Urology and Nephrology. 2019; 71: 457–478.

[21] Zanelli E, Giannarini G, Cereser L, Zuiani C, Como G, Pizzolitto S, *et al*. Head-to-head comparison between multiparametric MRI, the Partin tables, memorial Sloan Kettering cancer center nomogram, and CAPRA score in predicting extraprostatic cancer in patients undergoing radical prostatectomy. Journal of Magnetic Resonance Imaging. 2019; 50: 1604–1613.

[22] Offermann A, Hupe MC, Sailer V, Merseburger AS, Perner S. The new ISUP 2014/who 2016 prostate cancer grade group system: first résumé 5 years after introduction and systemic review of the literature. World Journal of Urology. 2020; 38: 657–662.

[23] Wang J, Huang B, Huang L, Zhang X, He P, Chen J. Prediction of extracapsular extension in prostate cancer using the Likert scale combined with clinical and pathological parameters. Frontiers in Oncology. 2023; 13: 1229552.

[24] Kunju LP, Daignault S, Wei JT, Shah RB. Multiple prostate cancer cores with different Gleason grades submitted in the same specimen container without specific site designation: should each core be assigned an individual Gleason score? Human Pathology. 2009; 40: 558–564.

[25] Rocco B, Sighinolfi MC, Sandri M, Eissa A, Elsherbiny A, Zoeir A, *et al*. Is extraprostatic extension of cancer predictable? A review of predictive tools and an external validation based on a large and a single center cohort of prostate cancer patients. Urology. 2019; 129: 8–20.

[26] Xu L, Zhang G, Zhang X, Bai X, Yan W, Xiao Y, *et al*. External validation of the extraprostatic extension grade on MRI and its incremental value to clinical models for assessing extraprostatic cancer. Frontiers in Oncology. 2021; 11: 655093.

[27] Kim SH, Cho SH, Kim WH, Kim HJ, Park JM, Kim GC, *et al*. Predictors of extraprostatic extension in patients with prostate cancer. Journal of Clinical Medicine. 2023; 12: 5321.

How to cite this article: Quan Ma, Wei Tian, Shasha Lv, Yongna Fu, Hui Wang, Jiansong He, *et al*. A nomogram for predicting extraprostatic extension in prostate cancer based on extraprostatic extension grade and clinical characteristics. Journal of Men's Health. 2024; 20(5): 48-56. doi: 10.22514/jomh.2024.070.